NIH Public Access
Author Manuscript
Z Med Phys. Author manuscript; available in PMC 2014 September 03.

Published in final edited form as:
Z Med Phys. 2012 December ; 22(4): 258–271. doi:10.1016/j.zemedi.2012.06.009.

Advances in 4D Radiation Therapy for Managing Respiration: Part I – 4D Imaging

Geoffrey D. Hugo[*] and **Mihaela Rosu**
Department of Radiation Oncology, Virginia Commonwealth University, Richmond, Virginia, USA

Abstract

Techniques for managing respiration during imaging and planning of radiation therapy are reviewed, concentrating on free-breathing (4D) approaches. First, we focus on detailing the historical development and basic operational principles of currently-available "first generation" 4D imaging modalities: 4D computed tomography, 4D cone beam computed tomography, 4D magnetic resonance imaging, and 4D positron emission tomography. Features and limitations of these first generation systems are described, including necessity of breathing surrogates for 4D image reconstruction, assumptions made in acquisition and reconstruction about the breathing pattern, and commonly-observed artifacts. Both established and developmental methods to deal with these limitations are detailed. Finally, strategies to construct 4D targets and images and, alternatively, to compress 4D information into static targets and images for radiation therapy planning are described.

Keywords

4D; radiation therapy; imaging; treatment planning; respiration management 4D; Strahlentherapie; bildgebende Verfahren; Bestrahlungsplanung; Atemmanagement

1 Introduction

Traditionally, the planning and delivery of radiation therapy has been conducted as if the patient were static over the several weeks of therapy. Although it has long been understood that this approximation is incorrect, technology was not available to deal with patient motion directly. Instead, a common strategy was to expand the target volume by a 'safety margin' to accommodate the estimated motion of the target volume, and to then irradiate larger fields under the expectation that this would compensate for the unknown motion. In the past two decades, imaging, planning, and delivery technology has progressed to the point that it is now possible to deal with a '4D' model of the patient, consisting of three spatial dimensions plus time as the fourth dimension.

All radiation therapy is inherently '4D', as planning and delivery cannot be accomplished instantaneously. Disparate processes such as abdominal organ motion induced by peristalsis and organ filling, and thoracic motion induced by respiration, all then fall under the general

[*]Corresponding author: 401 College St., P.O. Box 980058, Virginia Commonwealth University, Richmond, VA 23298, USA, (804) 628-7780, gdhugo@vcu.edu.

NIH-PA Author Manuscript
NIH-PA Author Manuscript
NIH-PA Author Manuscript

NIH-PA Author Manuscript

NIH-PA Author Manuscript

NIH-PA Author Manuscript

umbrella of ‘4D’, as time is a factor that must be considered during both planning and delivery of the treatment. However, the effects of different types of motion on the image of the patient and the dose distribution vary widely depending on a variety of factors such as the magnitude and shape of the motion, reproducibility of the motion during a single fraction and day to day, and proximity between moving targets and risk structures. For example, a head and neck cancer patient may swallow during irradiation, shifting the position of targets and risk structures. This type of motion may be dealt with by stopping delivery, and imaging and setting up the patient again. However, such motion is generally not predictable or periodic, and therefore it is difficult to model it and fold interventions robust to it into the treatment delivery dynamically. Conversely, respiratory-induced motion of lung cancer is quasi-periodic, relatively stable from minute to minute and day to day, and can be predicted to first order by a few seconds. Thus, researchers have had success in dynamically adapting the beam to the motion, through techniques such as beam gating and tracking.

Because there is no one solution to deal with the different types of motion encountered over all potential treatment sites, techniques to model and deal with the various types and magnitudes of temporal change in anatomy are necessarily specific to the site and type of motion. Thus, it would be difficult to provide a general but in-depth review of 4D imaging and planning methods for all sites. Instead, we have chosen to review 4D imaging and planning techniques for dealing with respiration since this area is the most mature and respiratory management has become very common in the field. To keep the focus on ‘4D’, rather than on respiratory management, we have concentrated on free-breathing strategies only (as opposed to breath hold or gated techniques). In this paper, we review 4D imaging, starting with the most commonly-used modality of 4D computed tomography (4DCT), commonly-observed issues and artifacts present in 4D imaging, and new techniques that have emerged in the last few years to combat these problems. In a companion paper, we review 4D planning techniques, including required ancillary technology and algorithms, strategies for dealing with breathing motion in dose calculation, plan design, and plan review, and clinical findings from implementation of 4D planning techniques.

Basic three-dimensional medical imaging acquisition and reconstruction principles are based on the assumption that the object being imaged is static over the course of the acquisition. Imaging moving anatomy (such as the thorax and upper abdomen during respiration) violates these principles resulting in the presence of artifacts in the reconstructed image. Artifacts, the specific appearance of which is dependent on the imaging modality, can lead to incorrect object position, shape, and size in the image, blurring or distortion of the object boundary, decrease in contrast resolution, and increased image noise.

Techniques to deal with artifacts induced by motion were first developed in cardiac imaging [1] to address the beating heart, and later transferred to the entire thorax to deal with respiration. The original intent of these methods was to suppress motion and artifact to produce a clear image of the anatomy for diagnostic applications. For such applications, the motion range and trajectory of anatomy is often not required information to aid in diagnosis and therefore not often measured. However, in radiation therapy applications, the motion pattern impacts target design and delivered dose, and is therefore necessary information to

NIH-PA Author Manuscript

NIH-PA Author Manuscript

NIH-PA Author Manuscript

generate an acceptable treatment plan. 4D imaging techniques developed specifically for radiation therapy applications have emerged to capture this information.

Most major imaging modalities have been augmented with 4D capabilities to enable motion assessment over the respiratory cycle. CT, being the main imaging modality for planning and guiding conformal radiation therapy, was the first target for 4D development in radiation therapy. The introduction of 4DCT into radiation therapy was quickly followed by 4D MRI, 4D cone beam CT (CBCT), and 4D PET.

2 4D Medical Imaging Modalities in Radiation Therapy

2.1 4DCT (diagnostic quality)

2.1.1 Historical development—Two major types of 4D imaging are available across modalities. In the first type, which we will term ‘continuous’ acquisition, images of the entire anatomy of interest are continually acquired as the patient breathes, forming a 2D or 3D plus time dataset. Examples of this type of acquisition include fluoroscopy (2D plus time) and 256-slice cine CT [2]. The requirement for continuous acquisition is that, for each frame, the entire image be acquired quickly (subsecond) to capture the intended breathing state. With this mode of acquisition, simultaneous measurement of a signal related to the breathing state of the patient is not required.

The second major type of 4D acquisition, which we will term ‘stacked’, requires partial images (e.g., reconstructed slices or partial sets of projections) from separate breathing cycles to be combined into a full volumetric image representing a breathing state. Stacked acquisition can be acquired prospectively (by gating the imager to acquire the partial image at only a particular breathing state) or retrospectively. For retrospective acquisition, a separate signal related to patient breathing state must be acquired simultaneously and synchronized with image acquisition. This respiratory signal is then used to sort the partial images into the correct breathing state. The partial images from each breathing state can then be combined into a single volumetric (3D) image of the breathing state. For stacks of image slices, this implies simply placing the slice in the correct physical location to form an image volume [3]. For a partial set of sorted projections, the image volume is formed by reconstruction from these projections [4]. For either prospective or retrospective stacked acquisition, constructing a true 4D image requires enough 3D images to represent breathing states over the entire respiratory cycle. As addressed in the planning section below, the definition of “enough” depends on the end application, but traditionally six to ten breathing state images are used for most applications. Historically, constructing this 4D image was more efficient using the retrospective method rather than the prospective one [3–8]. To obtain a 4D image with N breathing states requires N separate prospective gated acquisitions, whereas many 3D images at various breathing states can be reconstructed from a single retrospective acquisition.

Much early work on retrospective stacked acquisition was performed on single slice CT imagers [9, 10]. Scan times of five to ten minutes to cover the entire thorax were typical. The extension of retrospective 4D acquisition to multi-slice CT (longitudinal coverage of a

NIH-PA Author Manuscript

NIH-PA Author Manuscript

NIH-PA Author Manuscript

few centimeters) reduced scan times to under one minute [3–5, 7], which has resulted in the widespread use of this technology over the past few years.

At the same time as the development of 4D multi-slice CT, several groups and manufacturers were developing diagnostic cone beam CT scanners, with longitudinal scan coverage of 12.8 cm and 256 detector rows or more [2, 11]. Also possessing fast rotation times, these diagnostic cone beam scanners enable acquisition of continuous 4DCT in 'cine' mode, where the table sits at a fixed position and several acquisitions during multiple gantry rotations are made.

2.1.2 Basic Principles of Operation—Multi-slice 4DCT is acquired in one of two manners, either in 'cine' mode or 'helical' mode. In cine mode, the table position remains fixed, and a series of projections are acquired over multiple gantry rotations for at least the temporal length of one breathing cycle. The table position is then changed to move to the next portion of anatomy uncovered by the previous acquisition. Pan introduced a data sufficiency condition for 4DCT applying to both cine and helical modes [12]. This condition states that complete spatial and temporal coverage requires data acquisition at a particular table location for the duration of one breathing period plus the time for data sufficiency of conventional acquisition (one full rotation for a full scan reconstruction, or one half rotation plus the fan angle for a half or 'short' scan reconstruction). The total duration of scan acquisition at each table position in cine mode is $\tau_b + \tau_g$, where τ_b is the patient breathing period and τ_g is the time to complete one gantry rotation [12].

In helical mode, the table is continually moved as the gantry rotates and the scan acquisition takes place. The pitch, which is the ratio of the distance the table moves during one gantry rotation to the width of the collimated beam in the longitudinal direction, must be set such that a full set of projections can be acquired by the detector array for a single table position, over one breathing cycle. If the patient breathing cycle is long, this implies that the table must move more slowly, and the pitch must be smaller. The maximum pitch is given by [12]:

$$p \leq \frac{\tau_g}{\tau_b + C\tau_g} \quad (1)$$

where C is 1 for full scan and (180 + fan angle)/360 for half scan. Others omit the $C\tau_g$ term in the denominator [4].

Regardless of the scan mode, cine or helical, these recommendations assume a fixed breathing period. The breathing period for real patients may vary somewhat during the imaging session, so these recommendations should be considered minimum durations required to achieve data sufficiency. Typically, the breathing period over a minute or so is measured, and the longest breathing period during this observation period is selected so that data sufficiency is likely to be fulfilled.

2.1.3 Breathing signal surrogates—For stacked acquisitions in all 4D modalities, a separately-acquired respiratory signal is necessary to sort either the raw data or reconstructed images into 'bins' which are centered around the desired breathing state.

NIH-PA Author Manuscript

NIH-PA Author Manuscript

NIH-PA Author Manuscript

Depending on the modality, different surrogates are available. A variety of 'external' surrogates are available, including optical and physical (e.g., strain gauges around the abdomen) monitors of the patient surface [3, 9, 10], spirometry to measure inhaled and exhaled air volume [5], nasal thermometry [13].

Recently, the use of internal breathing surrogates for 4DCT has been adopted from initial work in gated MRI (discussed below). Both 'image-based' and 'data-based' internal surrogates have been introduced (Fig. 1). An image-based internal surrogate is identified from the reconstructed image, including body area [14], analysis of various metrics in regions of interest [15, 16], and image registration [17]. Data-based surrogates are formed by identifying a consistent anatomical feature or implanted fiducial marker in the raw data (sinogram), and using this to sort the raw projections into bins. Examples of data-based surrogates include the kymogram [18], which calculates a metric from the cranio-caudal location of the 'center of mass' (calculated from the pixel intensities) in the projection; the 'Amsterdam shroud' [19], which identifies the cranio-caudal position of high-contrast horizontal edges (such as the diaphragm apex) in the projections; and segmentation of fiducial markers [20]. Fig. 2 describes algorithmic details for two example databased breathing signals.

2.1.4 Issues with standard methods—Stacked acquisitions, being acquired over multiple breathing cycles, are generally based on the assumption that, for a given breathing state, the anatomy returns to the same position at each cycle. If this assumption is violated, inconsistencies in the data occur with can result in artifacts in the reconstructed image. Slice stacking acquisitions such as multi-slice 4DCT can exhibit disconnected anatomy in the slice direction due to breathing variability. Fig. 3 shows such typical artifacts for a multi-slice 4DCT. For multi-slice 4DCT, the pitch is dependent on the breathing cycle period. If the period during scan acquisition is shorter than that upon which the pitch is based, an artifact is unlikely, but the scan information at the end of the breathing cycle will not be used. This results in extra dose to the patient. If the period is longer than that presumed during scan parameter selection, some portion of the breathing cycle will not be reconstructed for that table position, resulting in data loss over a portion of the scan. One solution to this problem is to reduce the pitch, which will reduce the prevalence of cycle variation-induced artifact, but will also prolong the scan duration and result in an increase in patient dose.

Continuous acquisitions in diagnostic multi-slice CT scanners, as each image frame is acquired in a very short time and thus 'freezes' the motion, are not as prone to breathing cycle variation artifacts. Instead, if characterization of the patient's breathing pattern is important (for example, for creating safety margins encompassing motion), then enough cycles must be captured during continuous imaging to represent the mean and variation of the breathing cycle. For radiographic imaging, one must balance this requirement with patient dose requirements.

NIH-PA Author Manuscript

NIH-PA Author Manuscript

NIH-PA Author Manuscript

2.2 4DCBCT (onboard treatment units)

2.2.1 Historical Development—Linear accelerator manufacturers began mounting kilovoltage cone beam CT acquisition systems onboard accelerator gantries almost ten years ago to enable improved target localization for beam delivery. Shortly thereafter, methods for 4D cone beam CT (4DCBCT) acquisition and reconstruction were presented in the literature [19–21]. 4DCBCT acquisition is a 'stacked' technique, although the partial images acquired for this technique are raw data projections, rather than reconstructed image slices.

2.2.2 Basic Principles of Operation—4DCBCT is generally acquired at a single table position, since the longitudinal detector coverage is generally long enough to cover the anatomy without moving the table. Unlike enclosed scanners, the rotation speed of the gantry on accelerator-mounted CBCT systems is limited by International Electrotechnical Commission recommendations to no faster than one rotation per minute. A scan at this speed would result in angular coverage of approximately six degrees per second. For a typical breathing cycle with a period of five to six seconds, over thirty degrees of the scan would be acquired in a single breathing cycle. To obtain an accurate reconstruction, CBCT generally requires acquisition at a frequency of approximately one to two projections per degree. For 4DCBCT, this requirement implies the projections sorted into each breathing state must achieve this sampling rate or the image quality will be degraded.

Sonke et al. [19], Li et al. [20], and Lu et al. [22] independently investigated the effect of 4DCBCT scan parameters on adequacy of sampling and image quality. Reconstruction theory predicts that the angular spacing between projections affects both the spatial resolution and contrast resolution in the reconstructed image. In 3D reconstruction, increasing the detector frame rate will increase the angular frequency, however, these studies showed that this does not hold for 4DCBCT. Increasing the projection frame rate will not affect the angular coverage of the 4DCBCT scan (Fig. 4), but results only in a higher density of projections in a bunch, with each bunch spaced by an angle depending on the gantry rotation speed and patient's breathing cycle length. Instead, to ensure adequate angular sampling, the gantry speed should be reduced for longer breathing cycle lengths [22]. Lu et al. recommended an angular spacing of three degrees, resulting in a total scan time of 5.5 min for a half scan and 10 min for a full scan, for a typical breathing period of 5 s. In clinical practice, this scan length would be unacceptable if used routinely during a treatment fraction, so the angular spacing is reduced at the expense of image quality.

As cone beam reconstruction generally provides better image quality for equal angular spacing between projections, and to lower patient dose, the imaging frame rate can also be reduced. Lu et al. recommended a frame rate of $\frac{20}{\tau_b}$ frames per second for a ten state 4DCBCT reconstruction of ten breathing states. Altering the frame rate has the advantage of achieving similar number of projections per scan, and therefore similar image doses for all patients. For a 5 s breathing cycle length, scans with 66 to 272 projections per breathing state for a 10 state 4DCBCT reconstruction have been reported, compared to approximately 660 projections for a standard CBCT acquisition. However, the overall 4DCBCT acquisition contains 660 to 2720 projections, which would normally result in an increase of patient dose

NIH-PA Author Manuscript

NIH-PA Author Manuscript

NIH-PA Author Manuscript

by a factor of up to four. To counteract this effect, the output per projection is generally decreased for 4DCBCT. Together, the lower number of projections per image and lower output per projection results in lower image quality for the 4DCBCT compared to conventional CBCT.

2.2.3 Issues with standard methods—Projection stacking acquisitions are less prone to variations in periodicity, and exhibit different artifacts due to trajectory variations. Periodicity variations result in unequal angular spacing between projections. This issue can be partially overcome if angular-dependent weighting is used in the reconstruction [23]. Trajectory variations of the anatomy result in inconsistency between the projections. If enough projections per breathing state are available, this will result in residual blurring of the anatomy. With fewer projections, a variety of artifacts may be present, including view-aliasing (streaking) at high contrast boundaries and blurring.

As mentioned above, achieving adequate angular sampling of the projection space in 4DCBCT requires lengthening the scan duration, which is generally infeasible for clinical practice. Accepting the increased angular spacing of a shorter scan means the data sufficiency condition is not fulfilled. For typical filtered backprojection reconstruction [24], reducing the number of projections per breathing state results in increased structural noise such as view-aliasing artifact (streaking) in the image and reduced contrast resolution.

2.3 4DMRI

2.3.1 Historical Development and Principles of Operation—Measurement of thoracic motion with MRI for radiotherapy applications is less explored than with 4DCT. Termed ‘dynamic MRI’, fast 2D pulse sequences were used to acquire coronal or sagittal images at subsecond frame rates, resulting in a 2D plus time ‘continuous’ acquisition [25–30]. Although not truly 4D imaging, dynamic MRI provides good information on thoracic and upper abdominal motion, which is predominantly in the cranio-caudal direction. Plathow et al. found good agreement for lung and tumor motion between 2D- and 3D-dynamic MRI [31]. Also, acquisition of oblique planes aligned along the principal axis of motion or multiple 2D planes may better estimate 3D motion.

Investigation of true 4D MRI has been more limited, mainly due to the limited frequency at which full 3D volumes can be acquired on current generation scanners. Most 4D MRI consists of acquisition of a full 3D MRI of the region of interest in a short (subsecond) acquisition to generate a single breathing state image [31, 32]. Because the duration to acquire the full 3D volume takes several milliseconds, it is difficult to obtain more than a few images per breathing cycle currently. To overcome this limitation, other groups have developed a stacked approach, where stacks of cine MRI acquisitions are sorted and stacked into a 4D MRI image [14]. For dynamic MRI, ‘internal’ surrogates can be extracted directly from the image using the acquired 2D images themselves to identify surrogates for breathing state. Cai et al. used an estimate of body area in the 2D slices as a respiratory signal [14]. Other approaches include acquisition of a gated MRI at a single breathing state using a navigator, which is a short acquisition of a high-contrast boundary (such as the diaphragm apex) [33]. The high contrast boundary is detected in the navigator, and forms a 1D

NIH-PA Author Manuscript

NIH-PA Author Manuscript

NIH-PA Author Manuscript

respiratory signal. Interlacing the navigator acquisition with the main study acquisition triggers the main study acquisition at the appropriate breathing state.

2.3.2 Issues with Standard Methods—The advantages of dynamic MRI over 4DCT are better soft tissue contrast (potentially important for upper abdominal sites and gross disease of the hilum and mediastinum) and the ability to image long patient sessions and volunteers due to the lack of radiation dose. The temporal and spatial resolution of 4D MRI is currently worse than that of 4DCT, although the temporal resolution is rapidly improving [32]. Stacked acquisition of 4D MRI will exhibit similar issues as stacked acquisition of 4DCT; namely, that breathing variation may impact the consistency of data acquired during different breathing cycles. 4D MRI acquired as 3D dynamic MRI (successive full 3D acquisitions) can be acquired with temporal resolution of around 1s. To achieve this volume acquisition at clinical magnetic field strengths is difficult, but can be done by applying adaptive or reduced sampling of the *k*-space [31]. This is analogous to reducing the angular projection frequency in 4DCBCT, and similarly may degrade image quality. Furthermore, residual motion of the anatomy during the 3D acquisition can introduce artifacts into the image.

2.4 4DPET

2.4.1 Historical Development and Principles of Operation—Patient motion, including respiration, is known to not only affect the size and shape of the imaged lesion on PET images, but also to alter the measured standard uptake value (SUV), relative to the true value [34]. To account for such issues, 4D methods were developed and introduced to PET imaging in parallel to similar developments in 4DCT [8, 13, 35]. Prospective gated acquisition and retrospective stacked acquisition are both available. In prospective gated PET, the respiratory signal is monitored, and scan acquisition only takes place during a pre-determined breathing state for a pre-determined time window. Retrospective acquisition uses a ‘list mode’, where the acquisition is continuous, individual counts are tagged with the breathing state from a separate respiratory signal, and then sorted into separate bins for each breathing state to be reconstructed [36, 37].

Once joint PET/CT scanners were available capable of both 4DCT and 4D PET acquisition, the 4DCT was used to improve the attenuation correction of the 4D PET scan by applying either an average or a per-state attenuation correction [38–41].

Given the routine use of 4DCT or 4D MRI to describe the motion of the anatomy during the breathing cycle, there is some debate as to whether there is any benefit to the multiple breathing state information afforded by 4D PET. Instead, a motion-corrected PET image at a single breathing state may be sufficient, provided the acquisition time is long enough (for example, with a prospective gated acquisition) to obtain adequate signal to noise. If some dynamics of the PET signal were expected over the breathing cycle, 4D PET would be of interest, but this is not common with standard tracers. However, the necessity of 4D PET versus high quality single breathing phase PET is only beginning to be evaluated [42, 43].

2.4.2 Issues with Standard Methods—4D PET has related issues of scan duration and image quality as with 4DCT and 4D MRI. A 3D PET scan requires a minimum number of

NIH-PA Author Manuscript

NIH-PA Author Manuscript

NIH-PA Author Manuscript

counts (related to scan duration) to achieve good image quality with sufficient signal to noise. As in 4DCT, each breathing state theoretically requires this minimum duration and thus a balance must be made between image quality and scan duration. A reduced scan duration for each breathing state image results in higher image noise, which can result in apparent changes of SUV inside a tumor over the breathing cycle when in fact these changes are due to poor counting statistics.

2.5 Alternatives to 4D Imaging – Gated Imaging

Some applications do not require the acquisition of dynamic images over the entire breathing cycle, but rather images at only one breathing state or a range of states. An example is gated radiation therapy, where the beam is delivered only when the patient is in a specified state of breathing. Although gated images can be generated as a subset of a 4D image, for dose and time considerations it is sometimes advisable to acquire this subset directly. The most common method to do so is to prospectively gate the imaging with respiration. Gated imaging involves measuring the breathing surrogate signal, and triggering the imaging to occur only when the surrogate is in a pre-defined state. An example of the use of gated imaging is for treatment verification with cone beam CT. In this case, it is undesirable to collect data outside of the treatment gating window, so verification imaging is only collected within this window, and used to verify localization of the target. One advantage of gated imaging is that only the necessary images are collected, which often reduces patient imaging dose. For cine CT and MRI, gated imaging may be faster to acquire, as only a single 3D image is captured. However, for other modalities, gated imaging may not necessarily save time. For example, prospectively gated cone beam CT may be slower than 4DCBCT as the gantry rotation must stop while the patient is out of the gating window, and restart when the patient's breathing re-enters the window.

3 Emerging Strategies for Dealing with Residual 4D Artifacts

3.1 Advanced Image Acquisition and Reconstruction

A variety of approaches have been developed and tested in the last five to ten years to combat the effects of breathing cycle variation and sampling limitations mainly present in 4DCT, 4DCBCT, and 4D PET. These innovations can be separated into two broad classes. The first class seeks to dynamically adjust the acquisition to the patient's breathing cycle, adjusting parameters or gating the acquisition as the breathing pattern changes (or vice versa, coaching the patient to a reproducible breathing pattern). This class includes methods such as displacement/velocity gating [44–47], audio, visual, and audio-visual coaching [48–51], and altered data sorting methods [52–58]. The second class keeps the acquisition methods the same as the standard 4D acquisition, and either the data is modified in pre-processing prior to reconstruction or the reconstruction model itself is altered. This class includes a variety of methods including data-driven artifact suppression [59–62], use of a motion model for image reconstruction [63–82], and total-variation based iterative reconstruction algorithms [59, 83–89].

3.1.1 Amplitude sorting and other altered sorting methods—The main method of sorting 4DCT projection data into individual breathing state bins in conventional 4DCT and

NIH-PA Author Manuscript

NIH-PA Author Manuscript

NIH-PA Author Manuscript

4DCBCT is known as phase binning. In this method (Fig. 5), the breathing signal is assumed quasi-periodic and decomposed by phase. An easily-identified reference phase is selected (e.g., end of inhalation), and the breathing signal is divided into segments between each reference phase. This cycle segment is then mapped to the interval $[0,2\pi)$, where the zero phase is one reference phase and the 2π phase is the next occurrence of this phase (in the next cycle). Trajectory variations result in inconsistent locations of the same anatomy in different cycles, which results in inconsistent projections, leading to artifacts.

Amplitude sorting instead bins the breathing signal by the signal amplitude, rather than phase [55]. Pure amplitude sorting results in artifacts as well, for irregular breathing. One bin may contain only one or a few cycles worth of data, while others have data from each cycle (Fig. 5). Additionally, pure amplitude sorting loses the correlation between the breathing state image and physiological information (i.e., there is no longer one image purely representing 'end of inhalation'). For these reasons, recently phase and amplitude sorting have been combined into a hybrid approach where both amplitude and phase are used to sort the projections [55].

3.1.2 Displacement/velocity gating—Related to hybrid approaches combining amplitude and phase sorting, another method combines amplitude (displacement) and breathing signal velocity. Langner et al. found that a combination of amplitude and signal velocity could be used to identify irregular breathing patterns and prospectively gate, or pause, the scan acquisition when the patient's breathing signal differed from a reference signal by a certain tolerance[45, 47]. Once the patient's breathing was restored to the reference condition, the scan recommenced. Generally, one cannot always rely on the patient to spontaneously return to the reference condition, and some type of patient coaching or feedback may be required.

3.1.3 Audio-visual coaching—Besides modifying the scan parameters, a feedback-based approach can be used to help the patient maintain a consistent breathing cycle. Audio only [49, 90, 91], visual only [48], and combined audio-visual coaching [49] have been implemented, and shown to improve breathing reproducibility and image quality. These approaches require, though, external equipment and patient compliance. Also, if coaching is used during image acquisition, it should also be used during treatment delivery to reduce systematic errors (different breathing patterns during imaging used for treatment planning and during delivery).

3.1.4 Data-based artifact suppression—This class of 4D artifact reduction techniques seeks to modify the data itself to suppress artifacts. One example used for 4DCBCT is 'auto-adaptive phase correlation' [60]. In this method, the regions of static anatomy in the projection data are identified, and these regions are used in the reconstruction of all breathing state images. Other regions, identified as containing moving anatomy, are sorted into bins and reconstructed as in conventional 4D. While not improving the image quality in the moving regions, this method does improve quality and reduce view-aliasing in the static regions.

NIH-PA Author Manuscript

NIH-PA Author Manuscript

NIH-PA Author Manuscript

3.1.5 'Data-driven' motion models—In the past ten years, researchers began to realize that the trajectory of the anatomy in the thorax follows a generally reproducible pattern, and that tissue trajectories are well-correlated with the trajectories of adjacent regions of tissue. Thus, low-dimensional models of the motion of the thorax during respiration began to emerge [63, 66, 70, 80, 82, 92]. Although these models are often patient specific, good models can often be generated from low-quality 4D images and used to iteratively improve the image quality of a 4D acquisition. Alternatively, if a patient model exists already – for example, from a pre-treatment high-quality 4DCT or 4D MRI acquisition – it can be used as a prior in reconstructing a newly-acquired 4D image (for example, a 4DCBCT).

The modeling process itself is varied. A common method is to use principal components analysis (PCA) to decompose a high-dimensional set of breathing trajectories (e.g., known displacements of a large number of voxels in a reconstructed 4D image) into a small set of basis vectors, where each basis vector holds correlated components of the anatomical trajectories [66, 77, 81]. The basis vector model can then be used to either interpolate or extrapolate the position and trajectory of the anatomy over the breathing cycle. In a related method, Low et al. used spirometry to parameterize a low-dimensional model with inhaled and exhaled air volume and flow [92]. Finally, rather than a dynamic model, others have acquired a high-quality breath hold CT as a prior, and then registered or fit partial 4D scans to the high-quality model to generate a 4D motion model [70].

Several techniques have been developed to apply the motion model to reconstruct a 4D image. The most common method is termed 'motion-compensated image reconstruction', which assumes a fixed, periodic trajectory of the anatomy using the model. Motion-compensated reconstruction was developed in PET and SPECT [64, 69, 71–74, 78] to improve the signal to noise ratio, but has since been applied to 4DCBCT. In 4DCBCT, the model is used to either deform the projection data [75, 76] or the reconstructed breathing state image [67, 68] to a reference state, where the data or images are then summed to create a single, high-quality reconstruction. Presumably, one could then loop over all desired breathing states to create a 4D image, if desired. Fig. 6 shows an example of image quality improvements afforded by a motion-compensated reconstruction.

A second motion-model reconstruction technique, known by several terms but described here as 'projection to volume', iterates the underlying motion model to match the raw data [63, 77, 80, 93]. For each projection, the parameters of the underlying 4D motion model are iterated, and a synthetic model projection generated, until the measured projection and synthetic model projection are found to be of sufficient similarity. This method currently requires a simple (reduced parameter) 4D motion model, otherwise too many free parameters are present and the problem can be difficult to solve iteratively.

Motion-model approaches such as motion-compensated reconstruction and projection to volume have several advantages over conventional 4D imaging. By using the prior model, the sampling requirements of conventional 4D imaging can be overcome. Additionally, projection to volume does not use the raw data to directly reconstruct the image intensity. For 4DCBCT, this may allow one to avoid conventional CBCT image quality issues such as scatter and noise degrading soft tissue contrast. However, motion model-based

NIH-PA Author Manuscript

NIH-PA Author Manuscript

NIH-PA Author Manuscript

reconstruction is still in development. It remains to be seen whether these approaches will be accurate in conditions where the model differs greatly from the anatomy on the day of imaging. Also, application of motion model approaches to other sites of respiratory influence, such as the upper abdomen, is still relatively new [81, 82].

3.1.6 Iterative methods—For solving the view-aliasing problem of 4DCBCT and 4D MRI, several groups have explored various iterative image reconstruction algorithms, replacing the conventional filtered backprojection approach [59, 83–89]. Assuming that an image of the thoracic anatomy consists mainly of large regions of piecewise constant intensity separated by sharp gradients, an image of the gradients or 'edges' in the image will be sparse (e.g., most of the gradient image will be empty). Obviously, this assumption does not hold physically for tissue, but it often does hold for *images* of tissue. Under this assumption, a penalty term in the iterative reconstruction can be applied to enforce sparseness of the gradients in the image. This gradient sparseness quantity is termed the 'total variation' of the image. Total variation image reconstruction algorithms seek to minimize the total variation while balancing with the reconstructed image being consistent with the measured data. The advantage of this approach is that visually stunning images can be reconstructed with relative poorly-sampled 4D acquisitions. However, one impact of the total variation penalty is that small, high contrast structures such as pulmonary vessels, fiducial markers, and small airways can lose contrast [59].

The prior image constrained compressed sensing (PICCS) method combines a prior model and total variation penalty for improved 4DCBCT reconstruction [83–86]. In this method, a conventional CBCT reconstruction using all the available projection data from the scan is reconstructed and used as a prior image. The fidelity of the reconstructed image to the prior is evaluated along with the data fidelity and total variation, as in other total variation-penalized algorithms.

4 Structure Segmentation and Target Definition

4.1 4D target/risk structure construction

The main purposes of 4D imaging in radiation therapy are to accurately identify the shape, position, and trajectory of targets, risk structures, and other anatomy of interest, and to enable evaluation of the cumulative dose over the respiratory cycle. Here we focus on designing planning structures. In the part II companion paper, 4D dose calculation will be discussed. The type of 4D target and risk structures depends strongly on the type of 4D planning one is to perform. In this section, a few strategies will be described that cover a range of planning options.

4.1.1 Motion quantification—The most common and simplest means to compensate for respiratory motion is to define a motion envelope encompassing all locations of the structure over the breathing cycle, as measured from a 4D image. This motion envelope is also commonly termed the internal target volume (ITV). If a 4D image exists that contains enough breathing states to encompass the entire breathing cycle (normally 10 state images are used), then one can delineate the structure on each image, and then find the union of the structures on each state image. An alternative approach is to delineate the structure on a

NIH-PA Author Manuscript

NIH-PA Author Manuscript

NIH-PA Author Manuscript

single image, and use deformable registration to propagate the structure to the other datasets prior to taking the union [94, 95]. One must keep in mind that this motion envelope represents the extent of motion on the 4D image only, and does not incorporate directly any information about variation in the breathing cycle, cycle to cycle or day to day.

A simpler approach for high contrast structures of intensity higher than background is to use a maximum intensity projection (MIP) image, which is an image derived from the 4D image by finding the maximum intensity at a voxel location over all state images. For objects of intensity lower than background (e.g., liver tumors) an analogous image known as the minimum intensity projection (MinIP) can be used. Since the MIP represents the union of the structure in all state images directly, contouring the object in the MIP should directly provide the motion envelope. Several issues with MIP images (and MinIP images) should be considered. Care should be taken if the structure overlaps an object of similar contrast at some point in the respiratory cycle, as this may obscure the boundary of the structure in the MIP. Artifacts in 4D images may also introduce artifacts into the MIP image.

When using a motion envelope to quantify the extent of structure motion, one must not forget that other sources of variation also contribute to intra- and inter-fraction variation in structure position, including setup error, treatment response, anatomical variation in relation to bony anatomy, and other sources of motion such as digestion. Because these error sources should be summed in quadrature [96], it becomes difficult to directly add a safety margin for such sources to the motion envelope. Technically, it is more appropriate to define the extent and trajectory of structure motion (e.g., of the target centroid) and combine this error source with others in a composite safety margin [96].

4.1.2 Mid-ventilation—A planning image defines the location of target and risk structures and also commonly serves as a reference image for image-guided localization during delivery. This image must accurately represent the location of targets and risk structures during planning, and also must present information consistent with that obtained on board the treatment unit. One straightforward method to achieve an accurate and stable reference image is to reconstruct the image at the mid-ventilation position [54, 97–99]. Note that if the trajectory of the anatomy contains hysteresis (the path taken by the anatomy is different during inhale and exhale), then the mid-ventilation position may not physically exist in any of the conventionally-reconstructed state images. One can reconstruct the mid-ventilation image using image registration of the state images to a reference state image [98]. Alternatively, if hysteresis is small, one can select the closest state image as the mid-ventilation image. A third option is to average all the state images into an average CT image [100], although this average image will have blurring artifacts in regions of large motion and therefore may not be useful to delineate structures on directly.

5 Conclusions

4D imaging methods to manage periodic respiration are well-developed in a variety of key radiotherapy imaging modalities, and have been integrated for several years into routine clinical practice. However, many challenges in image quality due primarily to irregular respiration remain. Technological innovations in image reconstruction, scan acquisition, and

NIH-PA Author Manuscript

NIH-PA Author Manuscript

NIH-PA Author Manuscript

the developing idea of using prior patient information should aid in building better patient models with little increase in patient imaging dose. Accurate, efficient, and robust 4D patient models will be a key component in routine application of safe and efficient 4D methods in radiation therapy planning and delivery.

Acknowledgments

We would like to thank Matthias Söhn for assisting with literature review. This publication was made possible by grant number NIH P01CA116602 from the U.S. National Institutes of Health (NIH). Its contents are solely the responsibility of the authors and do not necessarily represent the official views of the NIH.

References

1. Kachelriess M, Ulzheimer S, Kalender WA. ECG-correlated imaging of the heart with subsecond multislice spiral CT. IEEE Trans Med Imaging. 2000; 19:888–901. [PubMed: 11127603]
2. Endo M, Tsunoo T, Kandatsu S, Tanada S, Aradate H, Saito Y. Four-dimensional computed tomography (4D CT)--concepts and preliminary development. Radiat Med. 2003; 21:17–22. [PubMed: 12801139]
3. Pan T, Lee TY, Rietzel E, Chen GT. 4D-CT imaging of a volume influenced by respiratory motion on multi-slice CT. Med Phys. 2004; 31:333–40. [PubMed: 15000619]
4. Keall PJ, Starkschall G, Shukla H, Forster KM, Ortiz V, Stevens CW, et al. Acquiring 4D thoracic CT scans using a multislice helical method. Phys Med Biol. 2004; 49:2053–67. [PubMed: 15214541]
5. Low DA, Nystrom M, Kalinin E, Parikh P, Dempsey JF, Bradley JD, et al. A method for the reconstruction of four-dimensional synchronized CT scans acquired during free breathing. Med Phys. 2003; 30:1254–63. [PubMed: 12852551]
6. Saito K, Saito M, Komatu S, Ohtomo K. Real-Time Four-dimensional Imaging of the Heart with Multi-Detector Row CT. Radiographics. 2003; 23:E8.
7. Rietzel E, Pan T, Chen GT. Four-dimensional computed tomography: image formation and clinical protocol. Med Phys. 2005; 32:874–89. [PubMed: 15895570]
8. Nehmeh SA, Erdi YE, Pan T, Pevsner A, Rosenzweig KE, Yorke E, et al. Four-dimensional (4D) PET/CT imaging of the thorax. Med Phys. 2004; 31:3179–86. [PubMed: 15651600]
9. Ford EC, Mageras GS, Yorke E, Ling CC. Respiration-correlated spiral CT: a method of measuring respiratory-induced anatomic motion for radiation treatment planning. Med Phys. 2003; 30:88–97. [PubMed: 12557983]
10. Vedam SS, Keall PJ, Kini VR, Mostafavi H, Shukla HP, Mohan R. Acquiring a four-dimensional computed tomography dataset using an external respiratory signal. Phys Med Biol. 2003; 48:45–62. [PubMed: 12564500]
11. Mori S, Endo M, Tsunoo T, Kandatsu S, Tanada S, Aradate H, et al. Physical performance evaluation of a 256-slice CT-scanner for four-dimensional imaging. Med Phys. 2004; 31:1348–56. [PubMed: 15259638]
12. Pan T. Comparison of helical and cine acquisitions for 4D-CT imaging with multislice CT. Med Phys. 2005; 32:627–34. [PubMed: 15789609]
13. Wolthaus JW, van Herk M, Muller SH, Belderbos JS, Lebesque JV, de Bois JA, et al. Fusion of respiration-correlated PET and CT scans: correlated lung tumour motion in anatomical and functional scans. Phys Med Biol. 2005; 50:1569–83. [PubMed: 15798344]
14. Cai J, Chang Z, Wang Z, Paul Segars W, Yin FF. Four-dimensional magnetic resonance imaging (4D-MRI) using image-based respiratory surrogate: A feasibility study. Med Phys. 2011; 38:6384. [PubMed: 22149822]
15. Gaede S, Carnes G, Yu E, Van Dyk J, Battista J, Lee TY. The use of CT density changes at internal tissue interfaces to correlate internal organ motion with an external surrogate. Phys Med Biol. 2009; 54:259–73. [PubMed: 19088386]

NIH-PA Author Manuscript NIH-PA Author Manuscript NIH-PA Author Manuscript

16. Li R, Lewis JH, Cervino LI, Jiang SB. 4D CT sorting based on patient internal anatomy. Phys Med Biol. 2009; 54:4821–33. [PubMed: 19622855]
17. Carnes G, Gaede S, Yu E, Van Dyk J, Battista J, Lee TY. A fully automated non-external marker 4D-CT sorting algorithm using a serial cine scanning protocol. Phys Med Biol. 2009; 54:2049–66. [PubMed: 19287079]
18. Kachelriess M, Sennst D-A, Maxlmoser W, Kalender WA. Kymogram detection and kymogram-correlated image reconstruction from subsecond spiral computed tomography scans of the heart. Med Phys. 2002; 29:1489–503. [PubMed: 12148730]
19. Sonke JJ, Zijp L, Remeijer P, van Herk M. Respiratory correlated cone beam CT. Med Phys. 2005; 32:1176–86. [PubMed: 15895601]
20. Li T, Xing L, Munro P, McGuinness C, Chao M, Yang Y, et al. Four-dimensional cone-beam computed tomography using an on-board imager. Med Phys. 2006; 33:3825–33. [PubMed: 17089847]
21. Dietrich L, Jetter S, Tucking T, Nill S, Oelfke U. Linac-integrated 4D cone beam CT: first experimental results. Phys Med Biol. 2006; 51:2939–52. [PubMed: 16723776]
22. Lu J, Guerrero TM, Munro P, Jeung A, Chi PC, Balter P, et al. Four-dimensional cone beam CT with adaptive gantry rotation and adaptive data sampling. Med Phys. 2007; 34:3520–9. [PubMed: 17926955]
23. Parker DL. Optimal short scan convolution reconstruction for fanbeam CT. Med Phys. 1982; 9:254–7. [PubMed: 7087912]
24. Feldkamp LA, Davis LC, Kress JW. Practical cone-beam algorithm. JOSA A. 1984; 1:612–9.
25. Shimizu S, Shirato H, Aoyama H, Hashimoto S, Nishioka T, Yamazaki A, et al. High-speed magnetic resonance imaging for four-dimensional treatment planning of conformal radiotherapy of moving body tumors. Int J Radiat Oncol Biol Phys. 2000; 48:471–4. [PubMed: 10974464]
26. Plathow C, Fink C, Ley S, Puderbach M, Eichinger M, Zuna I, et al. Measurement of tumor diameter-dependent mobility of lung tumors by dynamic MRI. Radiother Oncol. 2004; 73:349–54. [PubMed: 15588881]
27. Plathow C, Ley S, Fink C, Puderbach M, Hosch W, Schmahl A, et al. Analysis of intrathoracic tumor mobility during whole breathing cycle by dynamic MRI. Int J Radiat Oncol Biol Phys. 2004; 59:952–9. [PubMed: 15234028]
28. Plathow C, Ley S, Fink C, Puderbach M, Heilmann M, Zuna I, et al. Evaluation of chest motion and volumetry during the breathing cycle by dynamic MRI in healthy subjects: comparison with pulmonary function tests. Invest Radiol. 2004; 39:202–9. [PubMed: 15021323]
29. Plathow C, Zimmermann H, Fink C, Umathum R, Schobinger M, Huber P, et al. Influence of different breathing maneuvers on internal and external organ motion: use of fiducial markers in dynamic MRI. Int J Radiat Oncol Biol Phys. 2005; 62:238–45. [PubMed: 15850927]
30. Plathow C, Klopp M, Fink C, Sandner A, Hof H, Puderbach M, et al. Quantitative analysis of lung and tumour mobility: comparison of two time-resolved MRI sequences. Br J Radiol. 2005; 78:836–40. [PubMed: 16110107]
31. Plathow C, Schoebinger M, Herth F, Tuengerthal S, Meinzer H-P, Kauczor H-U. Estimation of pulmonary motion in healthy subjects and patients with intrathoracic tumors using 3D-dynamic MRI: initial results. Korean J Radiol. 2009; 10:559–67. [PubMed: 19885311]
32. Biederer J, Dinkel J, Remmert G, Jetter S, Nill S, Moser T, et al. 4D-Imaging of the lung: reproducibility of lesion size and displacement on helical CT, MRI, and cone beam CT in a ventilated ex vivo system. Int J Radiat Oncol Biol Phys. 2009; 73:919–26. [PubMed: 19215826]
33. McConnell MV, Khasgiwala VC, Savord BJ, Chen MH, Chuang ML, Edelman RR, et al. Prospective adaptive navigator correction for breath-hold MR coronary angiography. Magn Reson Med. 1997; 37:148–52. [PubMed: 8978644]
34. Erdi YE, Nehmeh SA, Pan T, Pevsner A, Rosenzweig KE, Mageras G, et al. The CT motion quantitation of lung lesions and its impact on PET-measured SUVs. J Nucl Med. 2004; 45:1287–92. [PubMed: 15299050]
35. Nehmeh SA, Erdi YE, Pan T, Yorke E, Mageras GS, Rosenzweig KE, et al. Quantitation of respiratory motion during 4D-PET/CT acquisition. Med Phys. 2004; 31:1333–8. [PubMed: 15259636]

NIH-PA Author Manuscript NIH-PA Author Manuscript NIH-PA Author Manuscript

36. Yan, J.; Planeta-Wilson, B.; Carson, RE. Direct 4D List Mode Parametric Reconstruction for PET with a Novel EM Algorithm. IEEE Nucl Sci Symp Conf Rec; 1997; 2008. p. 3625-8.
37. Grotus N, Reader AJ, Stute S, Rosenwald JC, Giraud P, Buvat I. Fully 4D list-mode reconstruction applied to respiratory-gated PET scans. Phys Med Biol. 2009; 54:1705–21. [PubMed: 19242055]
38. Pan T, Mawlawi O, Nehmeh SA, Erdi YE, Luo D, Liu HH, et al. Attenuation correction of PET images with respiration-averaged CT images in PET/CT. J Nucl Med. 2005; 46:1481–7. [PubMed: 16157531]
39. Nagel CC, Bosmans G, Dekker AL, Ollers MC, De Ruysscher DK, Lambin P, et al. Phased attenuation correction in respiration correlated computed tomography/positron emitted tomography. Med Phys. 2006; 33:1840–7. [PubMed: 16872091]
40. Chi PC, Mawlawi O, Nehmeh SA, Erdi YE, Balter PA, Luo D, et al. Design of respiration averaged CT for attenuation correction of the PET data from PET/CT. Med Phys. 2007; 34:2039–47. [PubMed: 17654907]
41. Rosario T, Ollers MC, Bosmans G, De Ruysscher D, Lambin P, Dekker A. Phased versus midventilation attenuation-corrected respiration-correlated PET for patients with non-small cell lung cancer. J Nucl Med Technol. 2009; 37:208–14. [PubMed: 19914979]
42. Ponisch F, Richter C, Just U, Enghardt W. Attenuation correction of four dimensional (4D) PET using phase-correlated 4D-computed tomography. Phys Med Biol. 2008; 53:N259–68. [PubMed: 18562779]
43. Aristophanous M, Yap JT, Killoran JH, Chen AB, Berbeco RI. Four-dimensional positron emission tomography: implications for dose painting of high-uptake regions. Int J Radiat Oncol Biol Phys. 2011; 80:900–8. [PubMed: 20950956]
44. Keall PJ, Vedam SS, George R, Williamson JF. Respiratory regularity gated 4D CT acquisition: concepts and proof of principle. Australas Phys Eng Sci Med. 2007; 30:211–20. [PubMed: 18044305]
45. Langner UW, Keall PJ. Prospective displacement and velocity-based cine 4D CT. Med Phys. 2008; 35:4501–12. [PubMed: 18975697]
46. Langner UW, Keall PJ. Accuracy in the localization of thoracic and abdominal tumors using respiratory displacement, velocity, and phase. Med Phys. 2009; 36:386–93. [PubMed: 19291977]
47. Langner UW, Keall PJ. Quantification of artifact reduction with real-time cine four-dimensional computed tomography acquisition methods. Int J Radiat Oncol Biol Phys. 2010; 76:1242–50. [PubMed: 19939579]
48. Cervino LI, Gupta S, Rose MA, Yashar C, Jiang SB. Using surface imaging and visual coaching to improve the reproducibility and stability of deep-inspiration breath hold for left-breast-cancer radiotherapy. Phys Med Biol. 2009; 54:6853–65. [PubMed: 19864703]
49. George R, Chung TD, Vedam SS, Ramakrishnan V, Mohan R, Weiss E, et al. Audiovisual biofeedback for respiratory-gated radiotherapy: impact of audio instruction and audio-visual biofeedback on respiratory-gated radiotherapy. Int J Radiat Oncol Biol Phys. 2006; 65:924–33. [PubMed: 16751075]
50. Masselli GM, Silvestri S, Ramella S, Trodella L. Design and evaluation of a methodology to perform personalized visual biofeedback for reducing respiratory amplitude in radiation treatment. Med Phys. 2009; 36:1467–72. [PubMed: 19544761]
51. Park YK, Kim S, Kim H, Kim IH, Lee K, Ye SJ. Quasi-breath-hold technique using personalized audio-visual biofeedback for respiratory motion management in radiotherapy. Med Phys. 2011; 38:3114–24. [PubMed: 21815385]
52. Abdelnour AF, Nehmeh SA, Pan T, Humm JL, Vernon P, Schoder H, et al. Phase and amplitude binning for 4D-CT imaging. Phys Med Biol. 2007; 52:3515–29. [PubMed: 17664557]
53. Gianoli C, Riboldi M, Spadea MF, Travaini LL, Ferrari M, Mei R, et al. A multiple points method for 4D CT image sorting. Med Phys. 2011; 38:656–67. [PubMed: 21452703]
54. Guckenberger M, Weininger M, Wilbert J, Richter A, Baier K, Krieger T, et al. Influence of retrospective sorting on image quality in respiratory correlated computed tomography. Radiother Oncol. 2007; 85:223–31. [PubMed: 17854931]

NIH-PA Author Manuscript NIH-PA Author Manuscript NIH-PA Author Manuscript

55. Lu W, Parikh PJ, Hubenschmidt JP, Bradley JD, Low DA. A comparison between amplitude sorting and phase-angle sorting using external respiratory measurement for 4D CT. Med Phys. 2006; 33:2964–74. [PubMed: 16964875]
56. Olsen JR, Lu W, Hubenschmidt JP, Nystrom MM, Klahr P, Bradley JD, et al. Effect of novel amplitude/phase binning algorithm on commercial four-dimensional computed tomography quality. Int J Radiat Oncol Biol Phys. 2008; 70:243–52. [PubMed: 18037590]
57. Wang J, Byrne J, Franquiz J, McGoron A. Evaluation of amplitude-based sorting algorithm to reduce lung tumor blurring in PET images using 4D NCAT phantom. Comput Methods Programs Biomed. 2007; 87:112–22. [PubMed: 17597250]
58. Wink N, Panknin C, Solberg TD. Phase versus amplitude sorting of 4D-CT data. J Appl Clin Med Phys. 2006; 7:77–85. [PubMed: 16518319]
59. Bergner F, Berkus T, Oelhafen M, Kunz P, Pa T, Grimmer R, et al. An investigation of 4D cone-beam CT algorithms for slowly rotating scanners. Med Phys. 2010; 37:5044–53. [PubMed: 20964224]
60. Bergner F, Berkus T, Oelhafen M, Kunz P, Pan T, Kachelriess M. Autoadaptive phase-correlated (AAPC) reconstruction for 4D CBCT. Med Phys. 2009; 36:5695–706. [PubMed: 20095282]
61. Bertram, M.; Rose, G.; Schäfer, D.; Wiegert, J.; Aach, T. Directional interpolation of sparsely sampled cone-beam CT sinogram data. Proceedings IEEE International Symposium on Biomedical Imaging (ISBI); 2004; p. 928-31.
62. Bertram M, Wiegert J, Schafer D, Aach T, Rose G. Directional view interpolation for compensation of sparse angular sampling in cone-beam CT. IEEE Transactions on Medical Imaging. 2009; 28:1011–22. [PubMed: 19131294]
63. Brock RS, Docef A, Murphy MJ. Reconstruction of a cone-beam CT image via forward iterative projection matching. Med Phys. 2010; 37:6212–20. [PubMed: 21302778]
64. Chang G, Chang T, Pan T, Clark JW Jr, Mawlawi OR. Joint correction of respiratory motion artifact and partial volume effect in lung/thoracic PET/CT imaging. Med Phys. 2010; 37:6221–32. [PubMed: 21302779]
65. Gao H, Cai JF, Shen Z, Zhao H. Robust principal component analysis-based four-dimensional computed tomography. Phys Med Biol. 2011; 56:3181–98. [PubMed: 21540490]
66. Li R, Lewis JH, Jia X, Zhao T, Liu W, Wuenschel S, et al. On a PCA-based lung motion model. Phys Med Biol. 2011; 56:6009–30. [PubMed: 21865624]
67. Li T, Koong A, Xing L. Enhanced 4D cone-beam CT with inter-phase motion model. Med Phys. 2007; 34:3688–95. [PubMed: 17926972]
68. Li T, Schreibmann E, Yang Y, Xing L. Motion correction for improved target localization with on-board cone-beam computed tomography. Phys Med Biol. 2006; 51:253–67. [PubMed: 16394337]
69. Li T, Thorndyke B, Schreibmann E, Yang Y, Xing L. Model-based image reconstruction for four-dimensional PET. Med Phys. 2006; 33:1288–98. [PubMed: 16752564]
70. McClelland JR, Blackall JM, Tarte S, Chandler AC, Hughes S, Ahmad S, et al. A continuous 4D motion model from multiple respiratory cycles for use in lung radiotherapy. Med Phys. 2006; 33:3348–58. [PubMed: 17022231]
71. Qiao F, Pan T, Clark JW Jr, Mawlawi O. Joint model of motion and anatomy for PET image reconstruction. Med Phys. 2007; 34:4626–39. [PubMed: 18196790]
72. Qiao F, Pan T, Clark JW Jr, Mawlawi OR. A motion-incorporated reconstruction method for gated PET studies. Phys Med Biol. 2006; 51:3769–83. [PubMed: 16861780]
73. Rahmim A, Tang J, Zaidi H. Four-dimensional (4D) image reconstruction strategies in dynamic PET: beyond conventional independent frame reconstruction. Med Phys. 2009; 36:3654–70. [PubMed: 19746799]
74. Reader AJ, Sureau FC, Comtat C, Trebossen R, Buvat I. Joint estimation of dynamic PET images and temporal basis functions using fully 4D ML-EM. Phys Med Biol. 2006; 51:5455–74. [PubMed: 17047263]
75. Rit S, Wolthaus J, van Herk M, Sonke JJ. On-the-fly motion-compensated cone-beam CT using an a priori motion model. Med Image Comput Comput Assist Interv. 2008; 11:729–36. [PubMed: 18979811]

NIH-PA Author Manuscript NIH-PA Author Manuscript NIH-PA Author Manuscript

76. Rit S, Wolthaus JW, van Herk M, Sonke JJ. On-the-fly motion-compensated cone-beam CT using an a priori model of the respiratory motion. Med Phys. 2009; 36:2283–96. [PubMed: 19610317]
77. Staub D, Docef A, Brock RS, Vaman C, Murphy MJ. 4D Cone-beam CT reconstruction using a motion model based on principal component analysis. Med Phys. 2011; 38:6697. [PubMed: 22149852]
78. Verhaeghe J, Gravel P, Mio R, Fukasawa R, Rosa-Neto P, Soucy JP, et al. Motion compensation for fully 4D PET reconstruction using PET superset data. Phys Med Biol. 2010; 55:4063–82. [PubMed: 20601774]
79. Yang D, Lu W, Low DA, Deasy JO, Hope AJ, El Naqa I. 4D-CT motion estimation using deformable image registration and 5D respiratory motion modeling. Med Phys. 2008; 35:4577–90. [PubMed: 18975704]
80. Zeng R, Fessler JA, Balter JM. Respiratory motion estimation from slowly rotating x-ray projections: theory and simulation. Med Phys. 2005; 32:984–91. [PubMed: 15895581]
81. Zhang Q, Hu YC, Liu F, Goodman K, Rosenzweig KE, Mageras GS. Correction of motion artifacts in cone-beam CT using a patient-specific respiratory motion model. Med Phys. 2010; 37:2901–9. [PubMed: 20632601]
82. Zhang Q, Pevsner A, Hertanto A, Hu YC, Rosenzweig KE, Ling CC, et al. A patient-specific respiratory model of anatomical motion for radiation treatment planning. Med Phys. 2007; 34:4772–81. [PubMed: 18196805]
83. Chen GH, Tang J, Leng S. Prior image constrained compressed sensing (PICCS): a method to accurately reconstruct dynamic CT images from highly undersampled projection data sets. Med Phys. 2008; 35:660–3. [PubMed: 18383687]
84. Leng S, Tang J, Zambelli J, Nett B, Tolakanahalli R, Chen GH. High temporal resolution and streak-free four-dimensional cone-beam computed tomography. Phys Med Biol. 2008; 53:5653–73. [PubMed: 18812650]
85. Qi Z, Chen GH. Extraction of tumor motion trajectories using PICCS-4DCBCT: a validation study. Med Phys. 2011; 38:5530–8. [PubMed: 21992371]
86. Qi Z, Chen GH. Performance studies of four-dimensional cone beam computed tomography. Phys Med Biol. 2011; 56:6709–21. [PubMed: 21965275]
87. Bian J, Siewerdsen JH, Han X, Sidky EY, Prince JL, Pelizzari CA, et al. Evaluation of sparse-view reconstruction from flat-panel-detector cone-beam CT. Phys Med Biol. 2010; 55:6575–99. [PubMed: 20962368]
88. Jia X, Lou Y, Li R, Song WY, Jiang SB. GPU-based fast cone beam CT reconstruction from undersampled and noisy projection data via total variation. Med Phys. 2010; 37:1757–60. [PubMed: 20443497]
89. Sidky EY, Pan X. Image reconstruction in circular cone-beam computed tomography by constrained, total-variation minimization. Phys Med Biol. 2008; 53:4777–807. [PubMed: 18701771]
90. Persson GF, Nygaard DE, Olsen M, Juhler-Nottrup T, Pedersen AN, Specht L, et al. Can audio coached 4D CT emulate free breathing during the treatment course? Acta Oncol. 2008; 47:1397–405. [PubMed: 18663648]
91. Haasbeek CJ, Spoelstra FO, Lagerwaard FJ, van Sornsen de Koste JR, Cuijpers JP, Slotman BJ, et al. Impact of audio-coaching on the position of lung tumors. Int J Radiat Oncol Biol Phys. 2008; 71:1118–23. [PubMed: 18258386]
92. Low DA, Parikh PJ, Lu W, Dempsey JF, Wahab SH, Hubenschmidt JP, et al. Novel breathing motion model for radiotherapy. Int J Radiat Oncol Biol Phys. 2005; 63:921–9. [PubMed: 16140468]
93. Li R, Jia X, Lewis JH, Gu X, Folkerts M, Men C, et al. Real-time volumetric image reconstruction and 3D tumor localization based on a single x-ray projection image for lung cancer radiotherapy. Med Phys. 2010; 37:2822–6. [PubMed: 20632593]
94. Sarrut D. Deformable registration for image-guided radiation therapy. Z Med Phys. 2006; 16:285–97. [PubMed: 17216754]

NIH-PA Author Manuscript

NIH-PA Author Manuscript

NIH-PA Author Manuscript

95. Werner R, Ehrhardt J, Schmidt-Richberg A, Albers D, Frenzel T, Petersen C, et al. Towards Accurate Dose Accumulation for Step-&-Shoot IMRT: Impact of Weighting Schemes and Temporal Image Resolution on the Estimation of Dosimetric Motion Effects. Z Med Phys. 2011

96. van Herk M, Witte M, van der Geer J, Schneider C, Lebesque JV. Biologic and physical fractionation effects of random geometric errors. Int J Radiat Oncol Biol Phys. 2003; 57:1460–71. [PubMed: 14630286]

97. Guckenberger M, Wilbert J, Krieger T, Richter A, Baier K, Flentje M. Mid-ventilation concept for mobile pulmonary tumors: internal tumor trajectory versus selective reconstruction of four-dimensional computed tomography frames based on external breathing motion. Int J Radiat Oncol Biol Phys. 2009; 74:602–9. [PubMed: 19427559]

98. Wolthaus JW, Schneider C, Sonke JJ, van Herk M, Belderbos JS, Rossi MM, et al. Mid-ventilation CT scan construction from four-dimensional respiration-correlated CT scans for radiotherapy planning of lung cancer patients. Int J Radiat Oncol Biol Phys. 2006; 65:1560–71. [PubMed: 16863933]

99. Wolthaus JW, Sonke JJ, van Herk M, Belderbos JS, Rossi MM, Lebesque JV, et al. Comparison of different strategies to use four-dimensional computed tomography in treatment planning for lung cancer patients. Int J Radiat Oncol Biol Phys. 2008; 70:1229–38. [PubMed: 18313530]

100. Glide-Hurst CK, Hugo GD, Liang J, Yan D. A simplified method of four-dimensional dose accumulation using the mean patient density representation. Med Phys. 2008; 35:5269–77. [PubMed: 19175086]

NIH-PA Author Manuscript

NIH-PA Author Manuscript

NIH-PA Author Manuscript

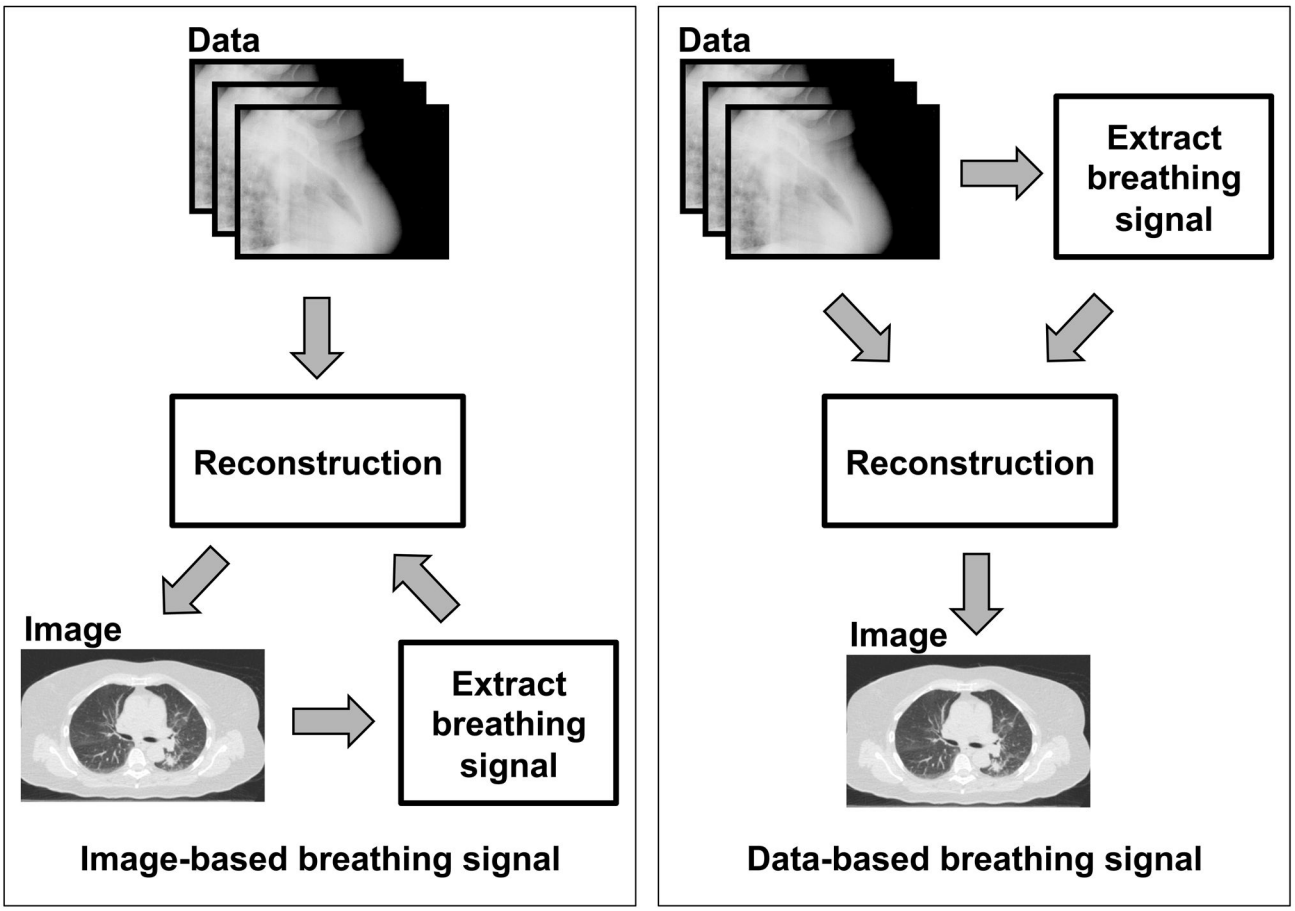

Figure 1.

Two main methods to extract an intrinsic breathing surrogate signal for forming 4DCT and 4D cone beam CT images. “Data” is the set of projections, “Image” is the reconstructed volumetric image. In the image-based methods, the image or a partial image is first reconstructed, and metrics such as edge intensity or body area are used to sort the projections or partial images into bins. The reconstruction process is repeated (or in the case of partial images, the partial images are reordered) to form the 4D image. In the data-based methods, the breathing signal is extracted directly from the projection data, and fed along with the projections into the reconstruction process.

NIH-PA Author Manuscript

NIH-PA Author Manuscript

NIH-PA Author Manuscript

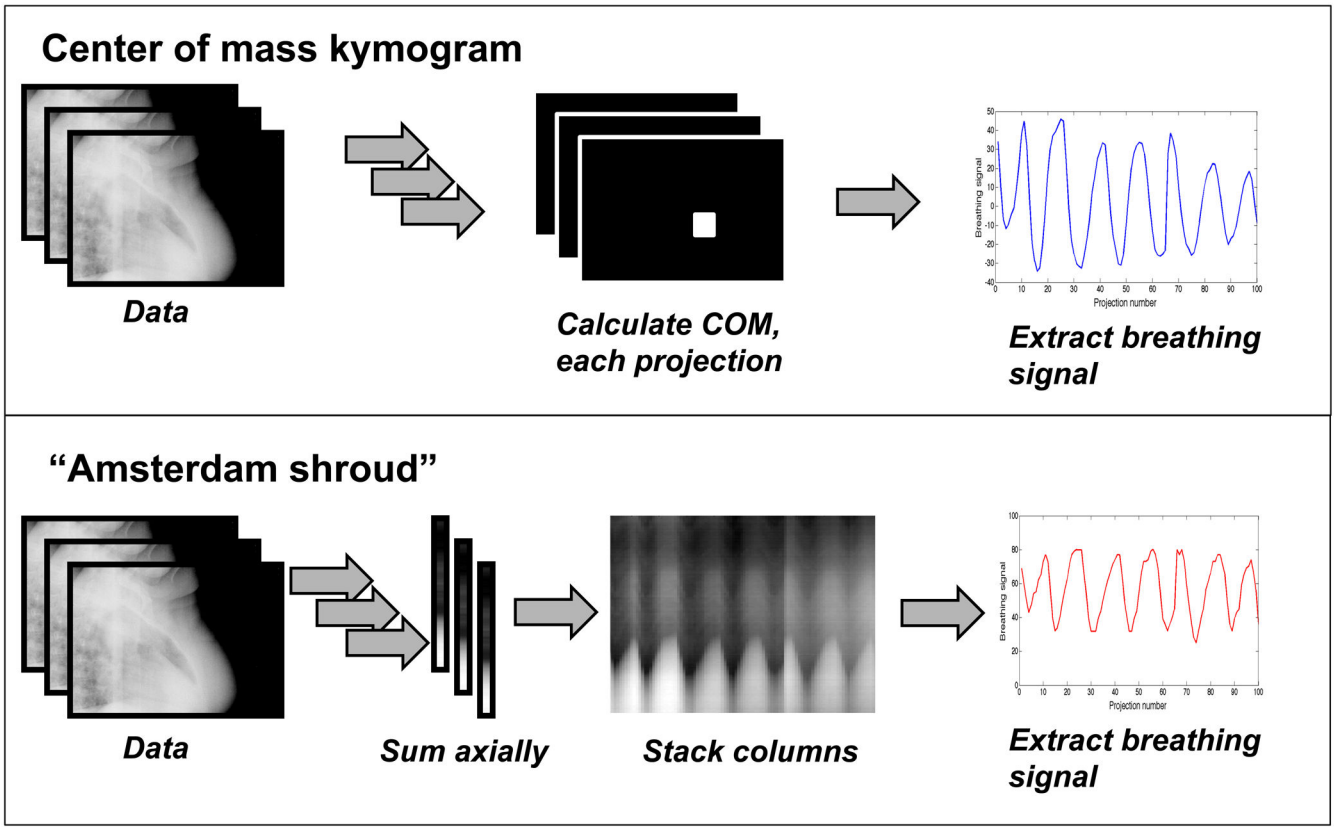

Figure 2.

Algorithms for two example data-based breathing signal extraction methods. For the center of mass (COM) kymogram, the center of mass is computed for each projection by calculating the average position of each pixel center weighted by the pixel intensity. The breathing signal is the cranio-caudal COM position as a function of projection number. For the "Amsterdam shroud" method, each projection is summed along the axial direction, resulting in a single column for each projection. The columns resulting from all projections are stacked to form a "shroud"; high contrast horizontal edges are enhanced in this image, and can be seen to form a breathing signal. The correlation between each two successive columns is computed and used to represent the breathing signal. Note that these two algorithms give similar, but not identical breathing signals for this single example clinical case.

NIH-PA Author Manuscript

NIH-PA Author Manuscript

NIH-PA Author Manuscript

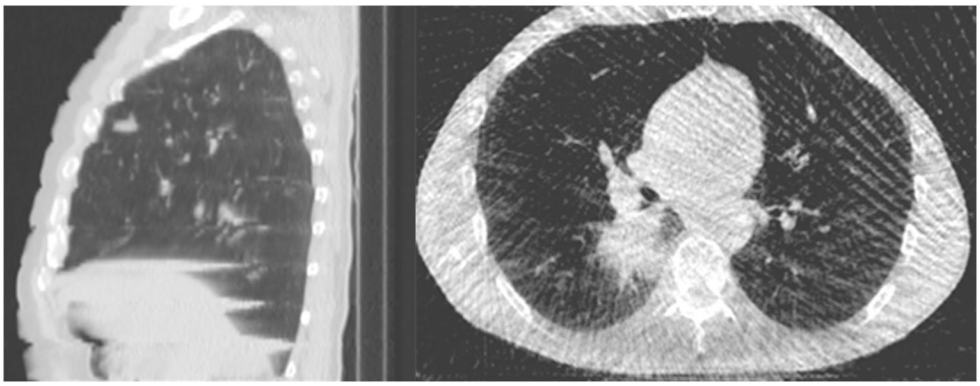

Figure 3.

Common artifacts in 4DCT and 4D cone beam CT (4DCBCT). Left, sagittal slice from a multi-slice 4DCT exhibiting artifact. These artifacts, visible at the diaphragm, chest wall, and patient surface, are caused by using too high a pitch for the breathing period of this patient. Right, axial slice from a 4DCBCT obtained with an onboard imaging system. View-aliasing (streaking) is evident due to inadequate angular sampling of the projections.

NIH-PA Author Manuscript

NIH-PA Author Manuscript

NIH-PA Author Manuscript

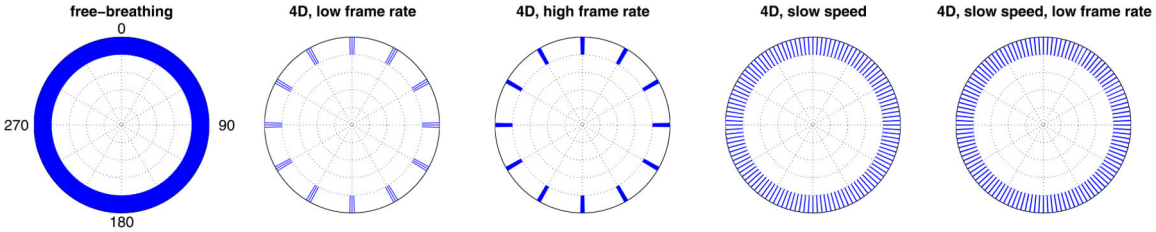

Figure 4.

Angular coverage for 4D cone beam CT (4DCBCT) acquisition. Each plot shows gantry angles at which projections are acquired. All scans assume a 5 s breathing period. The free-breathing scan shows a typical non-4D scan. The 4D scans show projections acquired only during the end of inhalation phase. Increasing the frame rate (the rate of acquisition of the projections) between the 'low frame rate' and 'high frame rate' scans does not improve the angular sampling, instead resulting in more projections in each 'bunch'. However, reducing the scan speed from one minute per revolution to ten minutes per revolution does improve the sampling. Finally, reducing both the speed and frame rate improves the sampling due to the speed reduction, and reduces the patient dose by decreasing the frame rate.

NIH-PA Author Manuscript

NIH-PA Author Manuscript

NIH-PA Author Manuscript

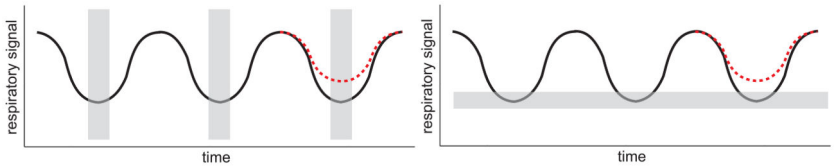

Figure 5.

Projection sorting for 4DCT. Left, phase sorting where projections are sorted only by phase of the breathing cycle. Right, amplitude sorting where projections are sorted by signal amplitude. For perfectly periodic and reproducible respiration, both methods work well. For irregular breathing cycles (shown by the dotted red line), simple phase sorting results in inconsistent projections due to the different position of the anatomy in different positions. For simple amplitude sorting, this inconsistency is avoided at the expense of loss of data during the irregular cycle as the signal does not enter the amplitude bin during this cycle.

NIH-PA Author Manuscript

NIH-PA Author Manuscript

NIH-PA Author Manuscript

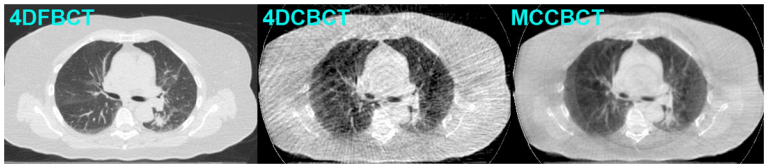

Figure 6.

Effect of motion-compensated reconstruction on 4D image quality. Left to right, a single phase from a 4D fan beam CT (4DFBCT), 4D cone beam CT (4DCBCT), and motion-compensated 4D cone beam CT (MCCBCT). Substantial view-aliasing (streak) artifact is evident in the 4D cone beam CT, which results in loss of contrast, particularly for smaller structures such as the pulmonary vessels. Motion-compensated reconstruction, which utilizes all projections rather than a subset at a particular phase, improves the overall quality at the expense of slight blurring. However, many of the small vessels seen in the 4D fan beam CT are recovered with the motion-compensated reconstruction.